

# Measurement of the radiographic anatomy of the small and ring metacarpals using computerized tomographic scans

Michael Rivlin<sup>1</sup> · Nayoung Kim<sup>1</sup> · Kevin F. Lutsky<sup>1</sup> · Pedro K. Beredjikian<sup>1</sup>

Published online: 5 May 2015  
© American Association for Hand Surgery 2015

## Abstract

**Background** To date, only plain radiographic definitions of normal anatomical parameters have been described. Our study aims to describe normal anatomic measurements of small and ring metacarpals using a novel digital reconstruction technique based on raw CT image data. We hypothesize that current plain radiographic data incorrectly describes normal metacarpal anatomy in the lateral plane.

**Methods** Thirty-five scans of the small and 30 scans of the ring metacarpals form the basis for this study. Using a custom digital 3D image reformatting software, CT sections were reconstructed in the plane of each studied metacarpal. The 3D images were converted to sagittal and coronal weighted projections to represent lateral and posteroanterior (PA) 2D images that are equivalent to “perfect orthogonal” radiographs. Using a customized image measurement program, shaft lengths, shaft-bending angle (SBA), and capital-axis angle (CAA) were measured.

**Results** Our results show that CAA averaged 14 and 12° in the ring and small metacarpals, respectively. Apex dorsal SBA averaged 12 and 10° in the ring and small metacarpals, respectively. On the PA images, the shafts are nearly straight. In contrast to prior reported values, we found the CAA to be less acute and the metacarpal curvature less pronounced on the lateral projection. We also demonstrated that much of the metacarpal apex dorsal bend is in the shaft itself.

**Conclusion** Normal anatomic parameters of metacarpals are based primarily on radiographic data, and as such are limited

due to bony overlap in the lateral plane, as well as imperfect radiographic projections that are known to distort anatomical relationships. This novel method of image reconstruction eliminates metacarpal overlap and defines precise anatomical reference for metacarpals.

**Keywords** Metacarpal anatomy · Metacarpal overlap · Metacarpal neck · 3D CT · Metacarpal imaging

## Introduction

Metacarpal neck fractures of the small and ring fingers typically occur as a result of a direct trauma. These injuries are common, with an incidence of 13.6 per 100,000 person-years for acute hospital care in the USA [8]. In addition, these fracture types account for 18 % of all hand injuries [4]. Indications for surgical treatment are based on the degree of fracture angulation and rotational alignment.

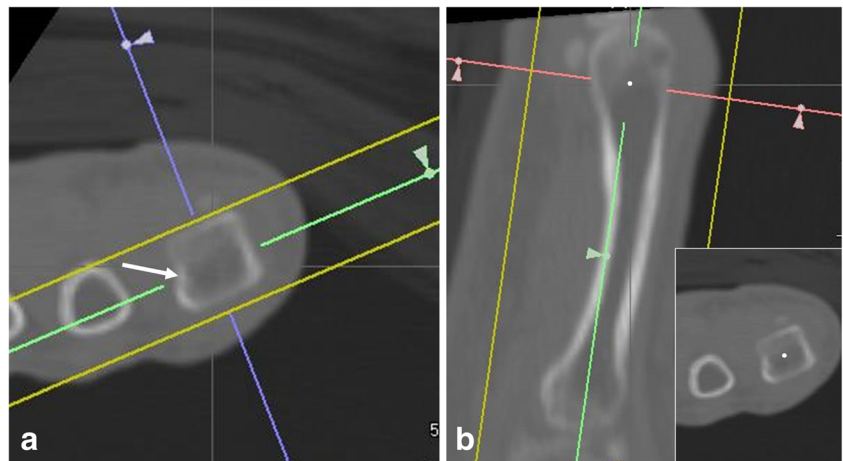
There is no consensus regarding a standard method of radiographic measurement of these fractures. Recent studies underscore the difficulty in reliably measuring the magnitude of displacement and angulation [5, 6, 10, 11]. Accurate measurement of deformity is important in assessing the extent of injury and determining an appropriate course of treatment [1, 2, 9]. Although some degree of deformity can be tolerated with little functional consequence, the goal of surgical treatment of metacarpal fractures is restoration of normal anatomy. As such, a good understanding of the normal anatomy is important in repairing or reconstructing metacarpal fractures.

There is a paucity of data detailing the normal radiographic anatomy, with only one report using plain radiographs to measure morphometric parameters. Due to bony overlap in the

✉ Michael Rivlin  
michael.rivlin@rothmaninstitute.com

<sup>1</sup> Rothman Institute of Orthopedics, Thomas Jefferson University, 925 Chestnut Street, 5th Floor, Philadelphia, PA 19107, USA

**Fig. 1** The process of defining the radiographic planes based on anatomical axis. 3D reconstruction of anatomical axis based on fine cut CT raw data points. **a** Line drawn perpendicular to the volar and dorsal cortices, bisecting the head (white arrow). **b** Line drawn from center point in the metacarpal head to the mid of the metacarpal base



lateral radiographic projection, our understanding of the metacarpal anatomy in this plane is significantly limited [2]. The purpose of this study is to describe the precise anatomy of normal small and ring metacarpals to serve as reference. We used a novel method of image manipulation of computer tomography (CT) images to eliminate difficulties inherent in measuring the anatomy in the lateral plane using radiograph, such as the overlap phenomenon.

## Methods and Materials

After the institutional review board approval of the project, 50 consecutive hand CT scans were identified retrospectively using a radiographic database. De-identified raw images from each scan were evaluated for adequate resolution, proper sequences, complete visualization of the metacarpals and no

obvious prior injury, severe arthritic changes, or other anomalies affecting the fourth and fifth metacarpals. Scans which were deemed inadequate based on these properties, or those in which there were any acute or chronic pathologic changes involving the small and ring metacarpals were excluded from study analysis.

Thirty-five scans of the small metacarpal and 30 scans of the ring metacarpal were included in this study. We aimed to power our study to discriminate  $5^\circ$  of change (paralleling the error range in measurement of conventional radiographs). To achieve this power, 15 scans were required. Doubling the required sample size allowed for the discrimination of nearly  $3^\circ$  of difference with statistical significance.

Using a digital 3D image reconstruction program (TeraRecon, Foster City, CA), the raw data point files from the CT scans were reconstructed in three planes [7, 12]. These planes

**Fig. 2** Virtual AP and lateral reconstructed X-rays (RaySum) in perfect projection



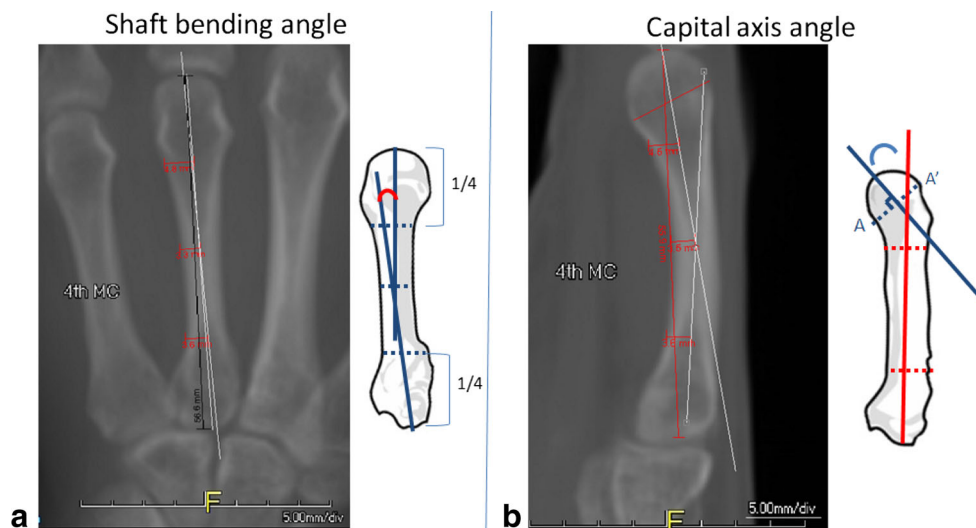


**Fig. 3** Measurement of shaft bending angle (SBA) and capital-axis angle (CAA). **a** The SBA was measured by drawing lines transversely that divided the metacarpal into four equal sections to establish the proximal, middle, and distal portions. A line was drawn from the midpoint of the proximal line to the midpoint of the middle line. Then a line was

drawn from the midpoint of the distal line to the midpoint of the middle line. The intersection of these two lines creates the SBA. **b** The CAA was found by drawing a line at the midpoint of the widest part of the cartilage cap and measuring the angle it makes to the metacarpal axis

were utilized to generate coronal and sagittal projections (RaySum) of each metacarpal individually based on the geometric axis of each bone. At the metacarpal head, a transverse (axial) line was drawn perpendicular to the volar and dorsal cortices and at the level of the radial collateral ligament recess, bisecting the head (Fig. 1a). Next, a line was drawn from this center point in the metacarpal head to the midpoint (anteroposterior (AP) and mediolateral) of the metacarpal base found on the axial view (Fig. 1b). From these, AP and lateral RaySum projections were constructed of the individual metacarpals within the field of view. This reconstruction produced virtual AP and lateral images of the individual digits (Fig. 2). All images were calibrated for size (pixel to distance calibration based on the radiographic marker and digital scale) to ensure accurate measurement.

Using an imaging measurement software (Rontgen Monogrammetric Analysis, Institute of Orthopaedics, Oswestry, UK), metacarpal anatomical relationships as defined by Braakman [2] were measured. The shaft lengths, shaft-bending angle (SBA), and capital-axis angle (CAA) were found on the lateral and AP views (Fig. 3). The SBA was measured by drawing lines transversely that divided the metacarpal into four equal sections to establish the proximal, middle, and distal portions. A line was drawn from the midpoint of the proximal line to the midpoint of the middle line.

**Table 1** Demographics

Average age (years)	47
Age range (years)	17–87
Male	22
Female	13
Total	35

Then a line was drawn from the midpoint of the distal line to the midpoint of the middle line. The intersection of these two lines creates the SBA (Fig. 3a). The CAA was found by drawing a line at the midpoint of the widest part of the cartilage cap and measuring the angle it makes to the metacarpal axis (Fig. 3b).

The shaft length was defined as the distance from the center of the most distal part of the distal condyle to the middle of the bony prominences at the metacarpal base and was measured on both coronal and sagittal images. The SBA is defined as the angle within the shaft of the metacarpal in the AP and lateral planes. By convention, radial bend (apex ulnar) was given a positive value, and ulnar bend (apex radial) was given a

**Table 2** Results

Averaged measurements	Fifth metacarpal		Fourth metacarpal	
	(mm)	SD	(mm)	SD
Metacarpal length	89	21	95	22
Proximal third diameter (lateral)	13	4	14	5
Distal third diameter (lateral)	16	4	16	4
Proximal third diameter (AP)	16	5	14	4
Distal third diameter (AP)	16	5	16	5
	(deg)	SD	(deg)	SD
Shaft bending angle (lateral)	10	3	12	3
Capital-axis angle (lateral)	12	6	14	12
Shaft bending angle (AP)	1	2	0	1
Radius of curvature (lateral)	256 mm		228 mm	

Angles: + = apex dorsa/apex radial

SD standard deviation

negative value. Similarly, volar bend was given a positive, while dorsal bend was given a negative value.

**Results**

The demographics of our study population are indicated in Table 1.

The measurements were tabulated and are summarized in Table 2. On average, the small metacarpals were 6 mm shorter than the ring metacarpals. There was no significant difference between the diameters of the ring and small metacarpals in their proximal and distal thirds. Shaft bending angles on the AP view demonstrate minimal angulation. This indicates that in the coronal plane, the metacarpals are essentially straight. However, in the sagittal plane, the metacarpals are not straight and as expected have an inherent bend. On the lateral view, the small

finger metacarpal is slightly straighter (SBA 10° vs ring SBA 12°). The small and ring metacarpals have comparable radii of curvature (215 mm for the small vs 213 mm for the ring). Figures 4a–d show the distribution of the CAA and SBA of the ring and small metacarpals in our study population.

Using computer simulation, 3D reconstruction of average metacarpal relationships may be modeled. Figure 5 demonstrates the mean anatomic relationships of the ring and small metacarpals.

**Discussion**

Metacarpal fractures are common injuries. An understanding of the normal anatomy of the metacarpals is important both in assessing injured hands and in reconstructing fractures and post-traumatic deformity. It has been demonstrated that

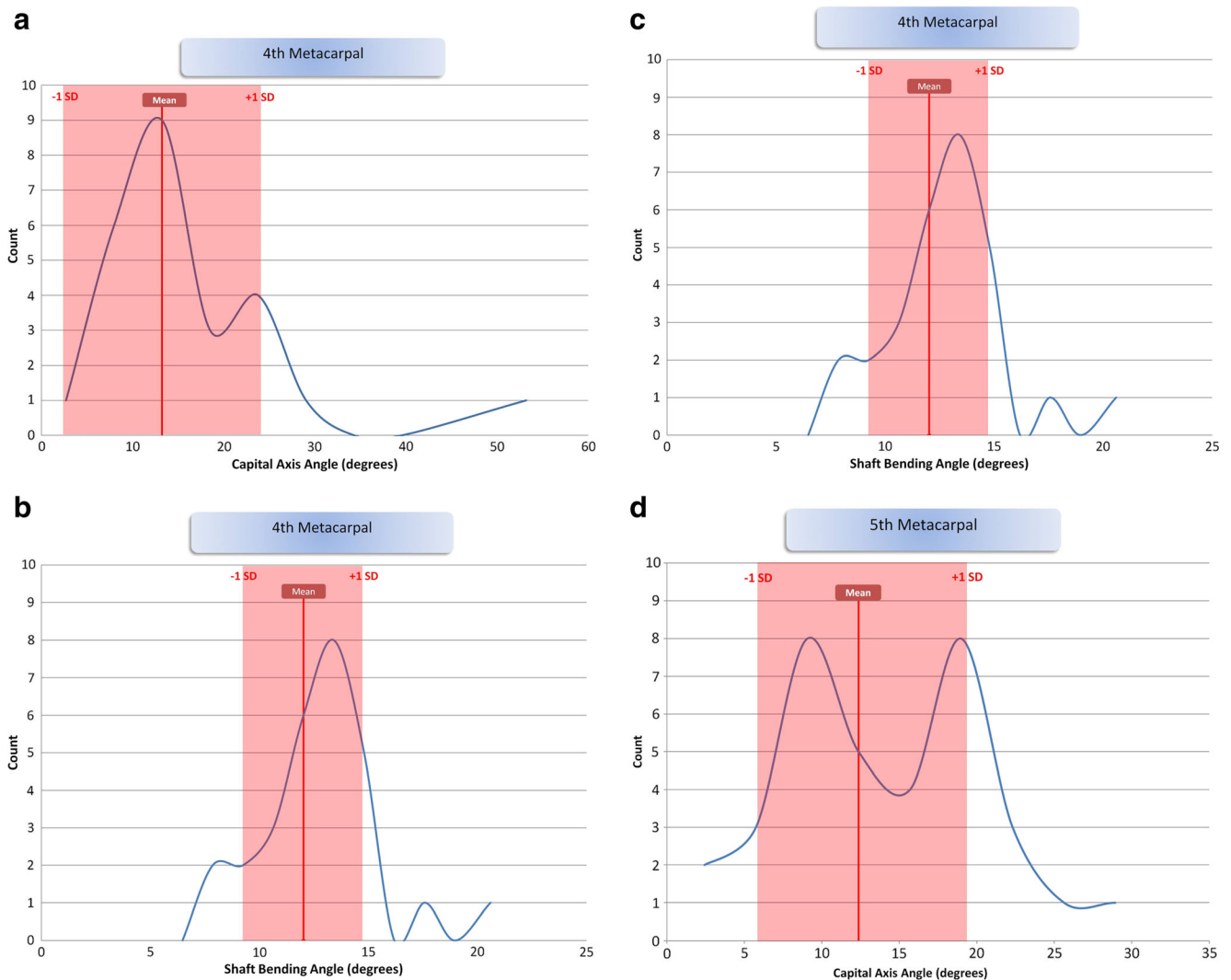
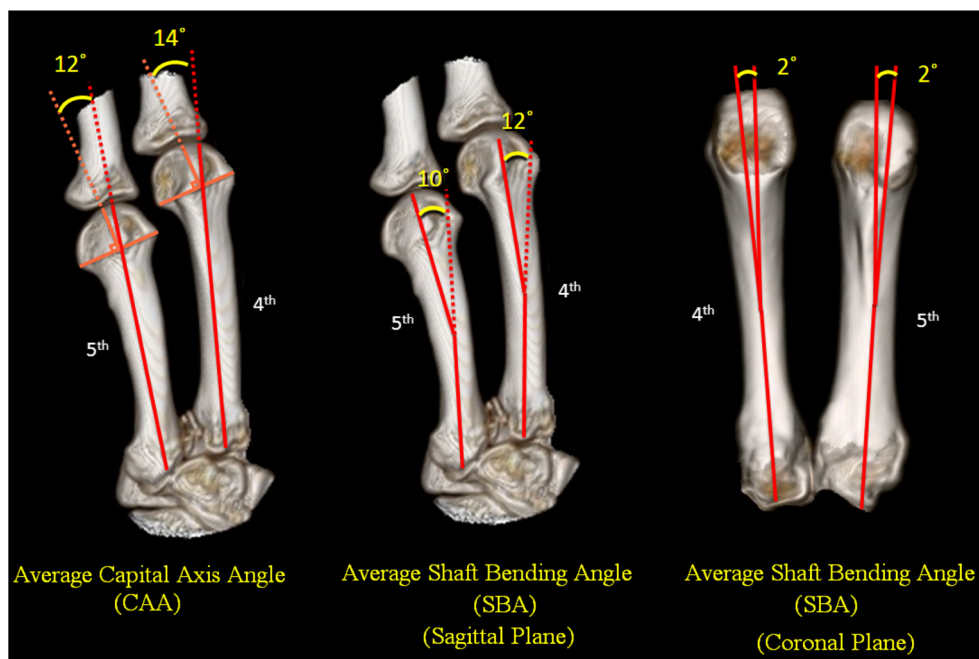


**Fig. 4 a–d** Distribution of measured relationships

**Fig. 5** Averaged anatomical model of metacarpal relationships



accurate evaluation of true metacarpal anatomy is difficult with conventional radiographs [5, 6, 10, 11]. Our current understanding of normal metacarpal anatomy is based on the work of Braakman et al. [2], who used radiographs to measure normal metacarpals. They measured capital and subcapital angulations, proximal articular inclination, and the shaft bending angles on PA and oblique radiographs to define normal values. In their study, CAA averaged 22 and 27° on the PA and 19 and 24° on the oblique radiographs for the ring and small metacarpals, respectively. They found that SBA was 2° in all tested digits in both projections. These measurements were not dependent on age, sex, or hand dominance in their study. Although our results were similar to theirs, we found the CAA to be less acute and the metacarpal curvature less pronounced. Our results show that CAA averaged 14 and 12° in the ring and small metacarpals, respectively, compared to 19 and 24° according to Braakman [2]. We also demonstrated that much of the metacarpal apex dorsal bend is in the shaft itself. SBA averaged 12 and 10° (apex dorsal on the “lateral view”) in the ring and small metacarpals, respectively. This relationship is important to consider when reconstructing metacarpals or when deciding how large a deformity is. Previous studies underestimate this relationship [2]. On the “true AP view,” the both metacarpal shafts are nearly straight. We found the SBA to be minimal, average 0 and 1° on the AP view in ring and small metacarpals, respectively (apex radial).

Knowledge of the normal dimensions and anatomic configuration of the ring and small metacarpals is valuable. First, it is important to have an understanding of normal metacarpal anatomy in assessing pathologic conditions such as fracture. Acceptable limits of angulation in ring and small metacarpal shaft fractures are 20–30 and 30–40°, respectively [3]. We

found that the metacarpals have an inherent apex dorsal bow, as evidenced by the 12° and 10° shaft bending angle of the ring and small metacarpals, respectively. Thus, any assessment of fracture angulation needs to take into account this alignment. Similarly, the metacarpal necks of the ring and small metacarpals are normally angulated 14 and 12°, respectively, apex dorsal. The overall posture of the metacarpal can be described as a gradual smooth bend in the shaft as well as an additional distal bend at the neck. A nondisplaced fracture may therefore still be associated with some degree of (normal) angulation. In the coronal plane, however, there is little inherent curvature to the metacarpal. Almost any degree of angulation in the coronal plane beyond a few degrees is likely to be abnormal.

Surgical correction of metacarpal fractures or malunions also requires knowledge of the normal anatomy. Anatomic reduction of a metacarpal neck or shaft fracture should account for the normal anatomical relationships including the gentle bow in the sagittal plane.

In post-traumatic reconstruction of massive bone loss from as gunshot wounds, infection, or tumor resection, knowledge of the normal dimensions of the metacarpals is critical to guide reconstruction. We found that the small metacarpal is, on average, 6 mm shorter than the adjacent ring metacarpal. Understanding this relationship may aid in the reconstruction of large deformities and bone defects.

Strengths of this study include the use of 3D reconstruction to measure the normal metacarpal anatomy. Radiographs of metacarpal anatomy can be difficult to measure accurately due to overlap of the adjacent metacarpals and variable rotation of the hand during positioning. True orthogonal views are difficult to obtain or standardize. By using CT scans, we were able

to maximize the accuracy and the radiological depiction of the anatomy and consistency in measurements. We reformatted the CT images rather than using the standard “sagittal cuts,” which inherently may not be in the plane of all the metacarpals. Reformats that are along the axis of the long bone lead to better resolution and more accurate measurement of geometric relationships.

All metacarpals examined were in isolated lateral or AP positions as a result of the reconstruction, a perspective that is nearly impossible to recreate using radiographs. We gained standardized radiographic projections as they relate to the anatomic parameters in the lateral plane and AP planes. Braakman’s [2] measurements may have been limited for this reason. Our reported results are free of the above distortions and represent anatomical relationships.

This study is limited by the relatively small study population that may not be a representative of the population in general, and this may introduce sampling bias. We did not stratify age differences, ethnicity, handedness, or different genders. Although evidence suggests minimal variation in metacarpal anatomy between men and women [2], it is presumable that men and women may have subtle differences in anatomy and this may skew our results.

The design of this study was based on a complicated 3D reconstruction model of determining metacarpal angulation and anatomy. We do not expect or intend that this model of measurement would be applicable to everyday clinical practice. Rather, we sought to provide a reliable clinical reference for the determination of anatomical parameters in the metacarpals. Further, a study of the index and long metacarpals would similarly be useful.

Our results can aid understanding the anatomical relationships in the ring and small metacarpals. The measured values for these bones can serve as reference for further investigations and clinical decision making. Knowledge of this anatomy is beneficial in evaluating and treating disorders of these rays.

**Acknowledgments** The authors would like to thank the contribution by Dr. Conor Shortt and Dr. Amy Austin for their dedication and help with image formatting and radiographic reconstruction of CT scans.

K.L. is a consultant for Synthes. P.B. has stock/stock options in Tornier, Inc. and receives payments for development of educational

presentations including service on speakers’ bureaus for Trimed, Inc. and gives expert testimony for malpractice/work compensation.

**Conflict of Interest** The authors have no conflict of interest relevant to this study.

**Statement of Human and Animal Rights** We obtained an institutional review board (IRB) approval from our university IRB and were waived of authorization to collect protected health information, or the requirement to obtain individual informed consent. All procedures followed were in accordance with the ethical standards of the responsible committee on human experimentation (institutional and national) and with the Helsinki Declaration of 1975, as revised in 2008.

## References

1. Beredjikian PK. Small finger metacarpal neck fractures. *J Hand Surg.* 2009;34:1524–6.
2. Braakman M, Verburg AD, Oderwald EE. Are routine radiographs during conservative treatment of fractures of the fourth and fifth metacarpals useful? *Acta Orthop Belg.* 1996;62:151–5.
3. Day C, Stern P. Fractures of the metacarpals and phalanges. In: Wolfe S, Hotchkiss R, Peterson W, Kozin S, editors. *Green’s operative hand surgery.* Philadelphia: Churchill Livingstone/Elsevier; 2011. p. 239–90.
4. Henry MH. Fractures of the proximal phalanx and metacarpals in the hand: preferred methods of stabilization. *J Am Acad Orthop Surg.* 2008;16:586–95.
5. Lamraski G et al. Reliability and validity of plain radiographs to assess angulation of small finger metacarpal neck fractures: human cadaveric study. *J Orthop Res.* 2006;24:37–45.
6. Leung YL et al. Radiographic assessment of small finger metacarpal neck fractures. *J Hand Surg.* 2002;27:443–8.
7. Mallee WH et al. Computed tomography for suspected scaphoid fractures: comparison of reformations in the plane of the wrist versus the long axis of the scaphoid. *Hand.* 2014;9:117–21.
8. Nakashian MN et al. Incidence of metacarpal fractures in the US population. *Hand.* 2012;7:426–30.
9. Ozturk I et al. Effects of fusion angle on functional results following non-operative treatment for fracture of the neck of the fifth metacarpal. *Injury.* 2008;39:1464–6.
10. Sletten IN et al. Assessment of volar angulation and shortening in 5th metacarpal neck fractures: an inter- and intra-observer validity and reliability study. *J Hand Surg Eur.* 2013;38:658–66.
11. Tasbas BA et al. Real angulation degree in fifth metacarpal neck fracture. *Eklemler hastaliklari ve cerrahisi=Joint Dis Relat Surg.* 2011;22:85–8.
12. Zannoni C, Cappello A, Viceconti M. Optimal CT scanning plan for long-bone 3-D reconstruction. *IEEE.* 1998;17:663–6.